Source, transport and impacts of a heavy dust event in the Yangtze River Delta, China in 2011

Xiao Fu [a,*], Shuxiao Wang [a, b,*], Zhen Cheng [a], Jia Xing [a, c], David Wang [c], Bin Zhao [a], Jiandong Wang [a], Jiming Hao [a, d]

[a] State Key Joint Laboratory of Environment Simulation and Pollution Control, School of Environment, Tsinghua University, Beijing 100084, China

[b] State Environmental Protection Key Laboratory of Sources and Control of Air Pollution Complex, Beijing 100084, China

[c] US Environmental Protection Agency, Research Triangle Park, NC, USA

[d] Collaborative Innovation Center for Regional Environmental Quality, Tsinghua University, Beijing 100084, China

*These authors contributed equally to this work

Correspondence to: S.X.Wang (shxwang@tsinghua.edu.cn)

Figure S1 shows the comparison of wind speed and wind direction between observations and predictions at the 3 monitoring sites. Bayan Dobo Suma in Mongolia (107.18E, 44.57N) is in the dust source region, Beijing (116.28E, 39.93N) is at the dust transport path and Shanghai (121.43E, 31.17N) is in the downwind region. The model can generally reproduce the variation trend of the observations. The bias of wind speed for these three sites are -2.13, -0.51 and -0.48 m/s respectively. The wind speeds are underestimated more in the source region than in the downwind region, which may result from the low resolution of the terrain at a coarse grid and less Data Assimilation (FDDA) data in the Mongolia region.

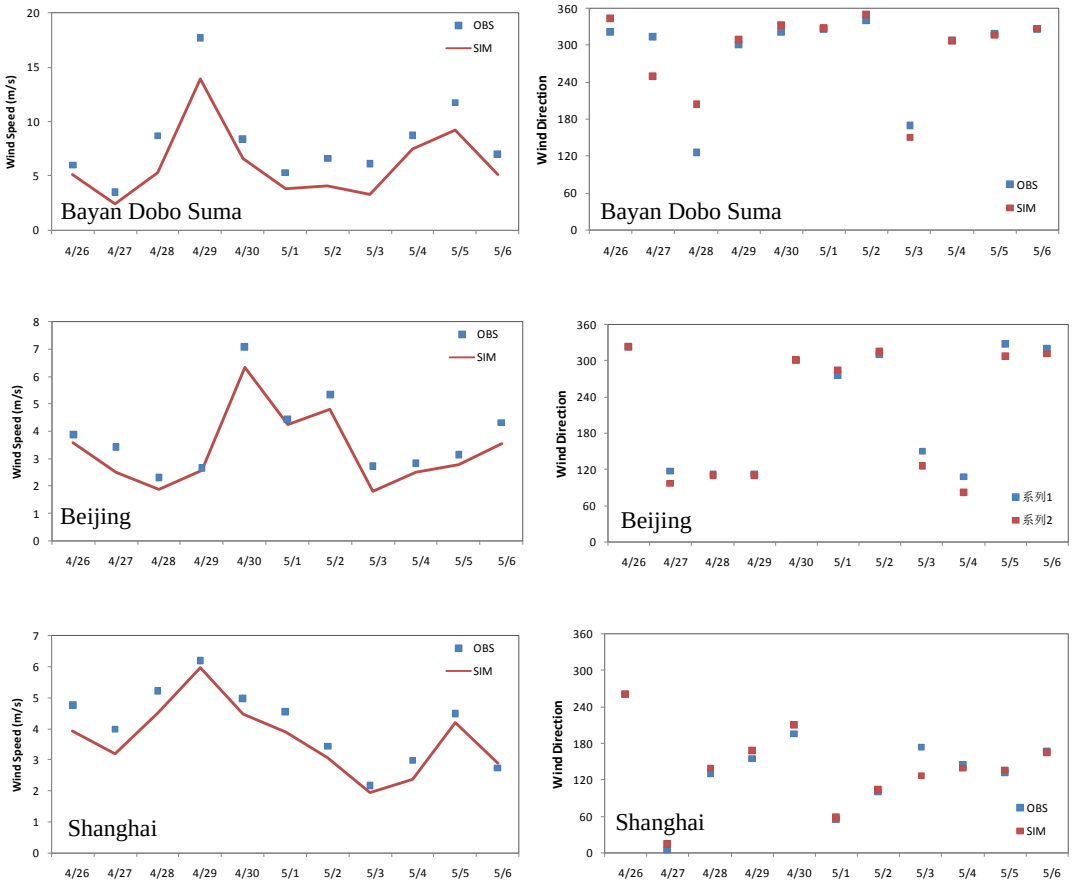

Fig. S1. The comparison of hourly wind speed and wind direction from observation and prediction at three sites

Figure S2 shows the comparison of the spatial distribution for the PM_{10} concentrations. In general, the spatial distribution of the observations was consistent with the simulations, especially near the source region (like 29 and 30 April). We can also see some overestimated cases at downwind regions. The possible reason is that the simulated results are average

values for 36km grid and it's difficult to capture the specific concentration for every point accurately for some time.

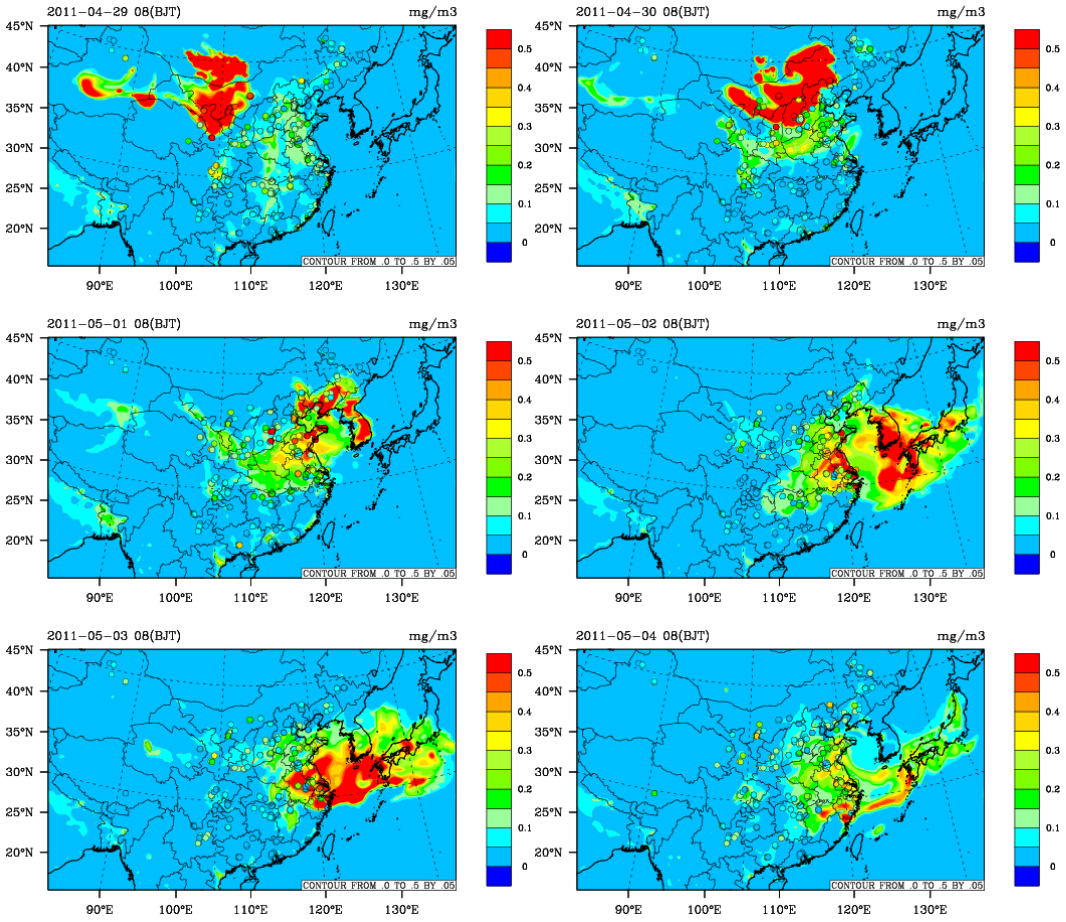

Fig.S2. Spatial distribution of the observed (the dots) and simulated (the contour) PM_{10} concentrations..

In order to test the model performance in terms of the ability to reproduce dust emission better, we compared PM_{10} concentration between observations and predictions at the 3 sites near source region, which include Baotou in Inner Mongolia (109.85E, 40.68N), Jinchang in Gansu (102.19E, 38.52N) and Yinchuan in Ningxia (106.17E, 38.48N). The comparison of observed and simulated hourly PM_{10} concentration is shown in the **Fig.S3**. Compared with DUST_DEFAULT and DUST_OFF, the model performance for DUST_REVISED is improved significantly. The NMBs for Baotou, Jinchang and Yinchuan are -22.2%, -38.6% and -50.4% averagely during 28 April to 6 May. The R values for these three sites are 0.77, 0.66 and 0.59, respectively. The revised model can generally capture the dust outbreak event during 29 and 30 April.

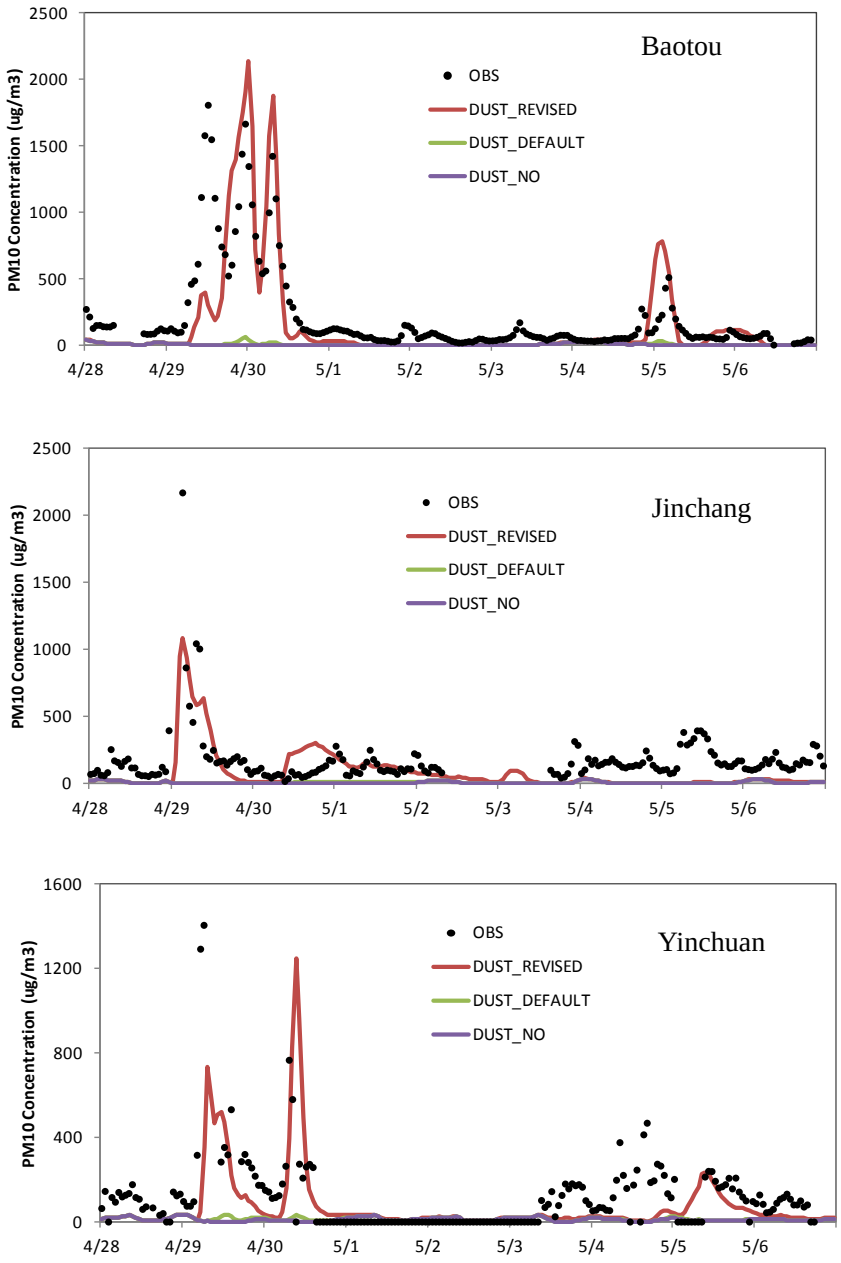

Fig. S3. The comparison of hourly PM_{10} concentration from observation and prediction with dust emission at three sites near dust source region

Figure S4 presents the daily averaged AOD distributions derived from simulation and retrieved from MODIS during the dust event. The comparison shows that the simulated AOD can generally catch the spatial distribution of satellite observation over Eastern China.

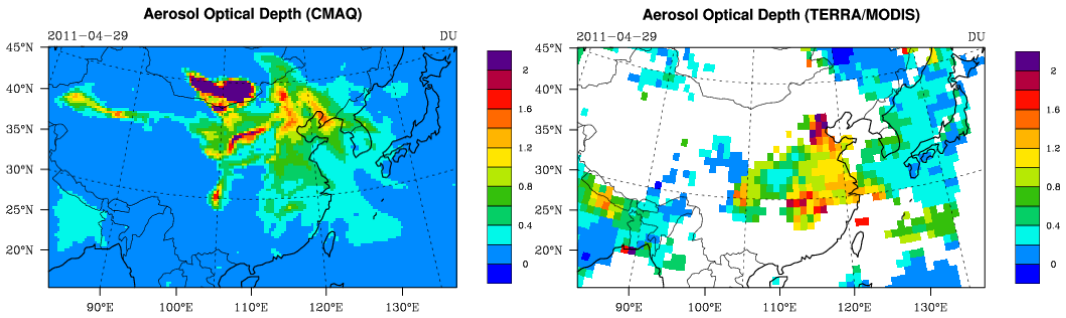
Aerosol Optical Depth (CMAQ)
2011-04-29
DU
45°N
40°N
35°N
30°N
25°N
20°N
90°E
100°E
110°E
120°E
130°E
2
1.6
1.2
0.8
0.4
0

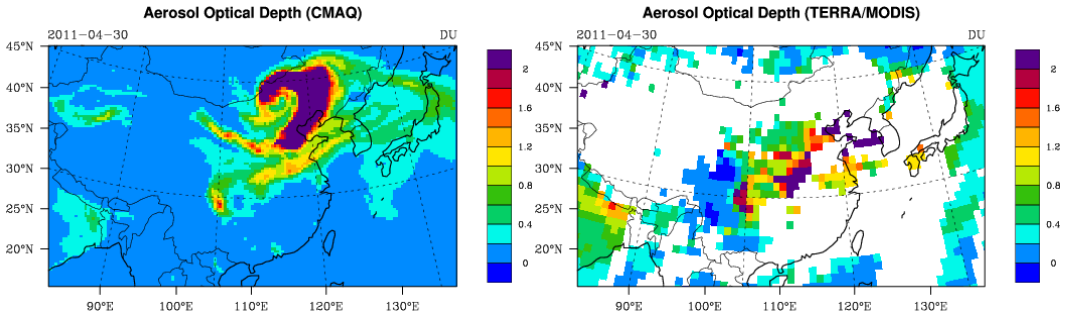
Aerosol Optical Depth (TERRA/MODIS)
2011-04-29
DU
45°N
40°N
35°N
30°N
25°N
20°N
90°E
100°E
110°E
120°E
130°E
2
1.6
1.2
0.8
0.4
0

Aerosol Optical Depth (CMAQ)
2011-04-30
DU
45°N
40°N
35°N
30°N
25°N
20°N
90°E
100°E
110°E
120°E
130°E
2
1.6
1.2
0.8
0.4
0

Aerosol Optical Depth (TERRA/MODIS)
2011-04-30
DU
45°N
40°N
35°N
30°N
25°N
20°N
90°E
100°E
110°E
120°E
130°E
2
1.6
1.2
0.8
0.4
0

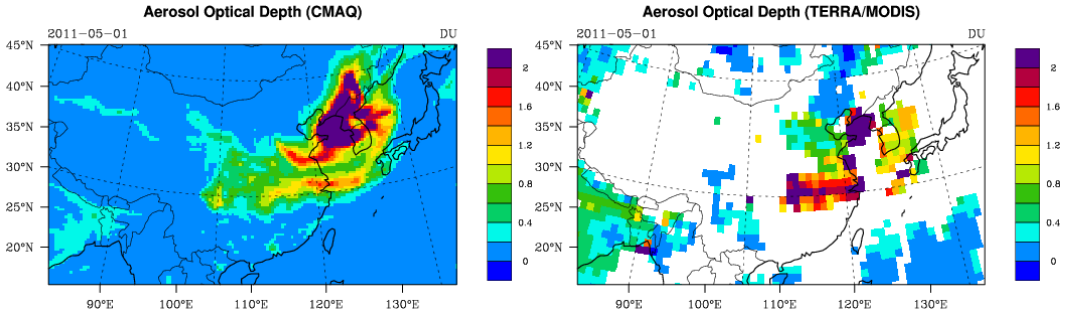
Aerosol Optical Depth (CMAQ)
2011-05-01
DU
45°N
40°N
35°N
30°N
25°N
20°N
90°E
100°E
110°E
120°E
130°E
2
1.6
1.2
0.8
0.4
0

Aerosol Optical Depth (TERRA/MODIS)
2011-05-01
DU
45°N
40°N
35°N
30°N
25°N
20°N
90°E
100°E
110°E
120°E
130°E
2
1.6
1.2
0.8
0.4
0

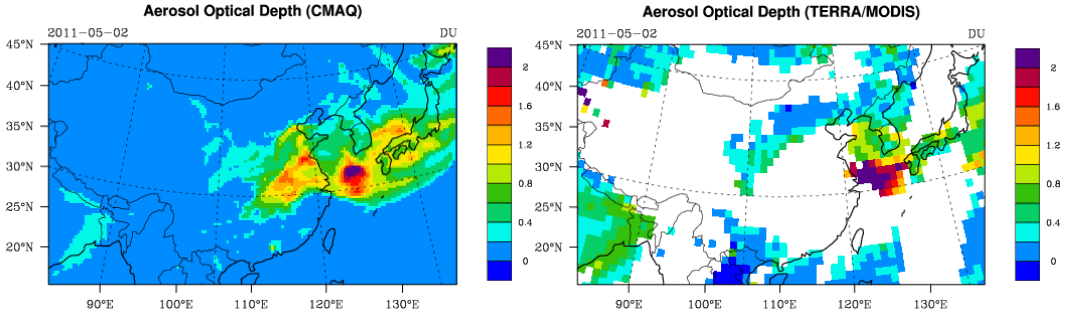
Aerosol Optical Depth (CMAQ)
2011-05-02
DU
45°N
40°N
35°N
30°N
25°N
20°N
90°E
100°E
110°E
120°E
130°E
2
1.6
1.2
0.8
0.4
0

Aerosol Optical Depth (TERRA/MODIS)
2011-05-02
DU
45°N
40°N
35°N
30°N
25°N
20°N
90°E
100°E
110°E
120°E
130°E
2
1.6
1.2
0.8
0.4
0

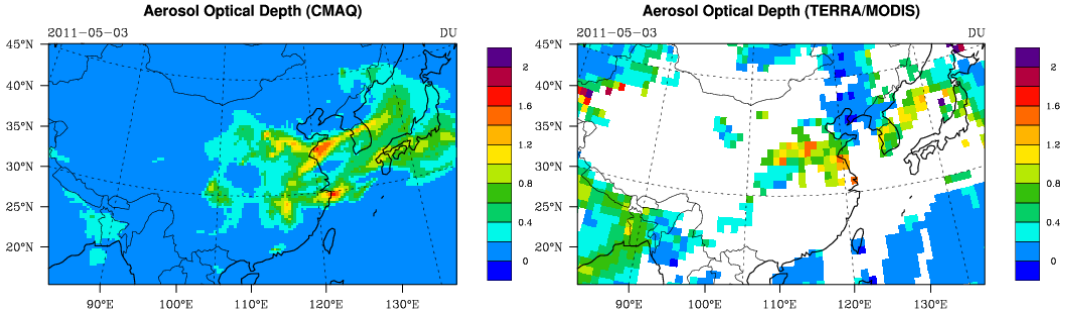
Aerosol Optical Depth (CMAQ)
2011-05-03
DU
45°N
40°N
35°N
30°N
25°N
20°N
90°E
100°E
110°E
120°E
130°E
2
1.6
1.2
0.8
0.4
0

Aerosol Optical Depth (TERRA/MODIS)
2011-05-03
DU
45°N
40°N
35°N
30°N
25°N
20°N
90°E
100°E
110°E
120°E
130°E
2
1.6
1.2
0.8
0.4
0

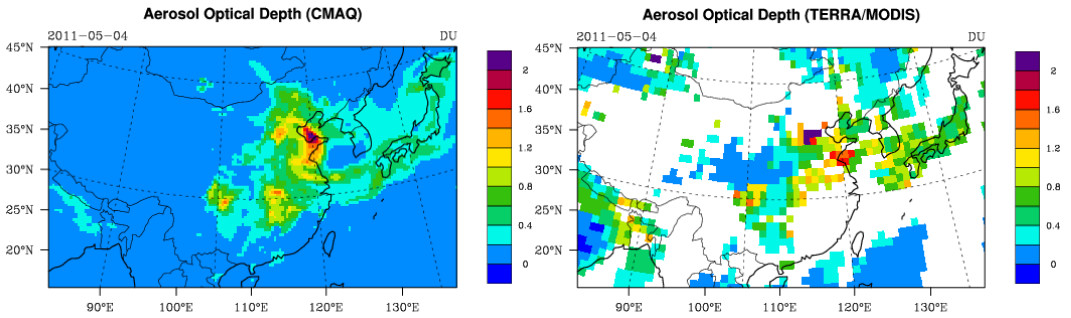

Fig.S4. Aerosol optical depth at 550 nm in 29 April to 4 May from model simulations (left) and from satellite measurements (right)

The distribution of simulated cloud fraction and precipitation during 1 to 6 May is shown as **Fig.S5**. It can be seen that there was little precipitation in the domain. The high values of cloud fraction and precipitation only occurred at the bottom of the domain. As the description in section 4.3, dust particles were transported from north to south, and then from sea to mainland, so the dust concentration was relatively low at the bottom of the domain. The distribution of wet deposition was generally similar with the distribution of precipitation.

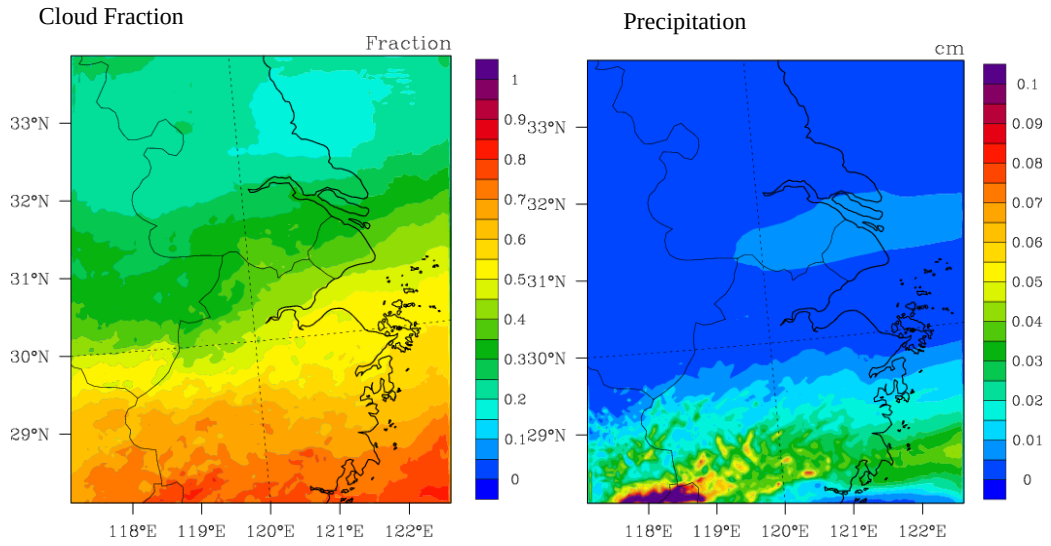

Fig. S5 Average cloud Fraction and precipitation distribution from 1 to 6 May